ARTICLE

Coherent Structures at a Forest Edge: Properties, Coupling and Impact of Secondary Circulations

Fabian Eder · Andrei Serafimovich · Thomas Foken

Abstract Little is known about the influence of coherent structures on the exchange process, mainly in the case of forest edges. Thus, in the framework of the ExchanGE processes in mountainous Regions (EGER) project, measurements of atmospheric turbulence were taken at different heights between a forest and an adjacent clear cutting using sonic anemometers and high-frequency optical gas analyzers. From these turbulence data, dominant coherent structures were extracted using an already existing wavelet methodology, which was developed for homogeneous forest canopies. The aim of this study is to highlight differences in properties of coherent structures between a forest and a clear cutting. Distinct features of coherent exchange at the forest edge are presented and a careful investigation of vertical and horizontal coupling by coherent structures around the surface heterogeneity is made. Within the forest, coherent structures are less frequent but possess larger time scales, indicating that only the largest coherent motions can penetrate through the forest canopy. At the forest edge, there is no crown layer that can hinder the vertical exchange of coherent structures, because these exhibit similar time scales at all heights. In contradiction to that, no improved vertical coupling was detected at the forest edge. This is mainly because the structures captured

F. Eder · A. Serafimovich · T. Foken
Department of Micrometeorology, University of Bayreuth, 95440 Bayreuth, Germany

Present Address:
F. Eder (✉)
Institute of Meteorology and Climate Research,
Atmospheric Environmental Research (IMK-IFU), Karlsruhe
Institute of Technology (KIT), Kreuzeckbahnstraße 19, 82467 Garmisch-Partenkirchen, Germany
e-mail: fabian.eder@kit.edu

Present Address:
A. Serafimovich
Helmholtz Centre Potsdam, GFZ German Research Centre for Geosciences, Telegrafenberg, 14473
Potsdam, Germany

T. Foken
Member of Bayreuth Centre of Ecology and Environmental Research (BayCEER), University of Bayreuth,
95440 Bayreuth, Germany

by the applied routine contribute less to total turbulent fluxes at the edge than within the forest. Thus, coherent structures with time scales between 10 and 40 s are not the dominant exchange mechanism at the forest edge. With respect to the horizontal direction, a consistent picture of coherent transport could be derived: along the forest edge there is mainly good coupling by coherent structures, whereas perpendicular to the forest edge there is mainly decoupling. Finally, it was found that there is a systematic modulation of coherent structures directly at the forest edge: strong ejection motions appear in all time series during the day-time, whereas strong sweeps dominate at night. An effect of wind direction relative to the forest edge is excluded. Consequently, it is hypothesized that this might be an indication of a quasi-stationary secondary circulation above the clear cutting that develops due to differences in surface temperature and roughness. Such circulations might be a relevant turbulent transport mechanism for ecosystem-atmosphere exchange in heterogeneous landscapes.

Keywords Coherent structures · Coupling processes · Forest edge · Wavelet analysis

1 Introduction

Turbulent flows have a considerable degree of order and consist of small-scale random motions as well as large-scale, organized, quasi-deterministic eddy structures (Cantwell 1981). These large-scale eddies are called coherent structures (Holmes et al. 1996). Coherence signifies that flow variables, such as wind velocity or temperature, exhibit high correlation with themselves and with each other. These correlations cover a range of space and time that is significantly larger than the scales of high-frequency random turbulence (Robinson 1991). The structures exist on a broad range of scales, so that it is crucial to define the object of investigation. In this study, in accordance with Thomas and Foken (2007b), coherent structures are defined as non-periodic, organized eddies in canopy flows, which appear as ramp structures in scalar time series and triangle-like patterns in vector time series.

Turbulence above high plant canopies, such as forests, largely differs from that in standard surface-layer flows. For a comprehensive review, see Finnigan (2000). In the so-called roughness sublayer above the canopy, turbulent diffusivities are larger than at an equivalent level in the atmospheric surface layer due to enhanced vertical mixing (Garratt 1978, 1980; Cellier and Brunet 1992). Within the forest, turbulence is highly intermittent and most of the transfer is restricted to distinct periods (Shaw et al. 1983; Finnigan 2000). Additionally, turbulent fluxes in the canopy do not follow local gradients (Denmead and Bradley 1985, 1987) and such counter-gradient fluxes can be also observed in the roughness sublayer (Fazu and Schwerdtfeger 1989). These findings suggest that coherent eddies of canopy scale play an important role in the exchange process between forest and atmosphere. Bergström and Högström (1989) and Gao et al. (1989) were the first to describe ramp structures within and above high plant canopies and highlighted the importance of coherent structures for the exchange process. According to the mixing-layer analogy (Raupach et al. 1996), these coherent structures develop from Kelvin–Helmholtz instabilities that form due to wind shear at the canopy top. Harman and Finnigan (2007, 2008) have developed a uniform description for profiles in tall plant canopies, which combines the theory of the roughness sublayer with the mixing-layer analogy. Besides the shear instability at canopy top, coherent structures in forest canopies can also be attributed to thermal plumes, which rise out of the canopy (Thomas et al. 2006). Furthermore, the occurrence of coherent structures in tall canopies can be related to larger coherent structures in the lower boundary layer that impinge down to the ground (Inagaki et al. 2012). However, Thomas and Foken (2007b) showed that the mixing-

layer analogy is valid to describe the fundamental properties of turbulence at the FLUXNET site 'Waldstein–Weidenbrunnen'. Accordingly, it is assumed that coherent structures above forest canopies are predominantly formed due to the presence of a mixing layer.

In order to extract such coherent motions from time series data, various methods have been developed. Because coherent structures cause strong fluctuations from the temporal mean, conditional sampling approaches (Antonia 1981) are useful tools to extract such structures from a time series. Firstly, laboratory (e.g. Kline et al. 1967; Lu and Willmarth 1973) and field experiments (e.g. Finnigan 1979; Bergström and Högström 1989; Gao et al. 1989) have shown that coherent structures mainly consist of a gradual lift-up, called an ejection, which is followed by a sudden burst, called a sweep. Wavelet analysis (Grossmann and Morlet 1984; Kronland-Martinet et al. 1987; Grossmann et al. 1989) is a powerful tool to develop automated detection algorithms in order to investigate large datasets. By using wavelet analysis for conditional sampling of coherent structures, Collineau and Brunet (1993a,b) developed a framework that is able to determine their time scales and flux contributions in tall plant canopies. Thomas and Foken (2005, 2007a,b) advanced this concept. Because coherent structures are supposed to play an important role in the exchange process between forest and atmosphere, Thomas and Foken (2007a) defined vertical coupling regimes between different canopy layers based on the flux contributions of coherent structures at different heights. Serafimovich et al. (2011b) extended this approach to the horizontal direction in order to investigate the lateral propagation of coherent structures in the trunk space of forests.

Up to now, numerous studies described coherent exchange in horizontally homogeneous forests, so that a brief summary on the general findings is appropriate. Such organized structures usually exhibit time scales of several tens of seconds, while their flux contribution depends on the sampling algorithm and it seems that coherent structures contribute in a greater fraction to scalar fluxes than to the momentum flux (Collineau and Brunet 1993b; Thomas and Foken 2007a; Serafimovich et al. 2011b; Steiner et al. 2012). With respect to plant canopies with a dense crown layer, the ejection is the dominant part of the coherent structure in the roughness sublayer, whereas the sweep dominates within the canopy layer (Finnigan 1979; Bergström and Högström 1989; Poggi et al. 2004; Katul et al. 2006). These motions can be directly linked to ecosystem responses such as sub-canopy respiration events (Zeeman et al. 2013).The vertical coupling by coherent structures is usually stronger during daytime than at night (Thomas and Foken 2007a; Serafimovich et al. 2011b), whereas horizontal coupling is mainly controlled by topography, vegetation structure and mean wind direction (Serafimovich et al. 2011b).

However, most forest sites are not homogeneous in the lateral direction. Forests reveal a rather patchy structure due to wind throws, forest fires and fragmented land use, while forest edges represent huge obstacles that might have a considerable impact on turbulent exchange.

Between different surfaces, quasi-stationary secondary circulations might develop (Mahrt 2010) and that might be relevant for the so-called energy balance closure problem (Foken 2008b; Mahrt 2010; Foken et al. 2012a). Theoretically, the available energy at the earth's surface, which can be derived from the net radiation (Q_S^*) and ground heat flux (Q_G), should be balanced by turbulent fluxes of sensible (Q_H) and latent heat (Q_E). Eddy-covariance measurements underestimate Q_H and Q_E, which results in a residual Res of the energy balance, which may be on the order of about 20 % of the available energy (Aubinet et al. 2000; Wilson et al. 2002),

$$Res = Q_S^* - Q_G - Q_H - Q_E. \tag{1}$$

Many possible reasons for the lack of energy balance closure have been discussed in the literature. To date, it is assumed that surface heterogeneities play a key role, either because

they cause the development of secondary circulations that are not routinely captured by eddy-covariance systems, or because it is directly in the region of surface heterogeneities where the "missing" fluxes can be found (Foken 2008b; Mahrt 2010; Foken et al. 2012a). Enhanced vertical turbulent fluxes have been determined in the downwind region of forest edges (Klaassen et al. 2002; Leclerc et al. 2003); these flux enhancements might be carried by additional coherent motions forming at the edge (Zhang et al. 2007).

Unfortunately, there is a lack of experimental data on turbulence around roughness heterogeneities so far. Sogachev et al. (2005, 2008) investigated the effects of forest edges and source distribution on flux estimates from eddy-covariance measurements above forests. Furthermore, there are several large-eddy simulations occasionally conducted together with measurements, which consider turbulent transport around forest edges and downwind from them (e.g. Yang et al. 2006a,b; Cassiani et al. 2008; Detto et al. 2008; Dupont and Brunet 2009; Huang et al. 2011; Dupont et al. 2012; Schlegel et al. 2012). However, these studies either did not explicitly focus on coherent transport or did not investigate properties of coherent structures directly at the edge.

In order to fill this gap, high-frequency turbulence measurements were conducted directly at a forest edge for several weeks in order to provide an extensive database. The relevant atmospheric exchange mechanisms at surface heterogeneities were detected and quantified, and the study attempts to

i. identify differences in properties of coherent structures (time scales, length scales, coherent flux contributions) between forest, forest edge and an adjacent clear cutting;
ii. compare the vertical coupling by coherent structures at a forest edge to the vertical coupling within a nearby forest;
iii. investigate the horizontal coupling by coherent structures along a forest edge and between a forest and a clear cutting.
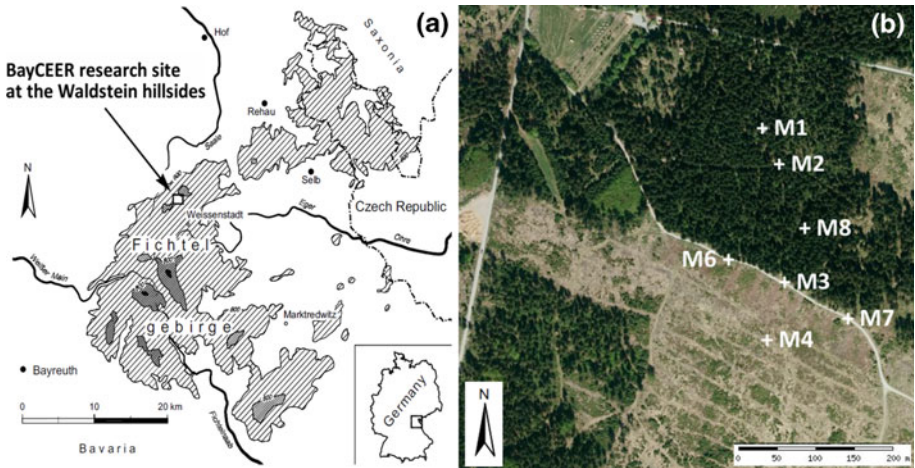
2 Experimental Set-up

2.1 Description of the Research Site

The experimental data were collected during the third intensive observation period (IOP3) of the ExchanGE processes in mountainous Regions (EGER) project (Foken et al. 2012b), which was conducted from June 13 to 27, 2011. The project aims at capturing the relevant exchange processes within the soil-vegetation-atmosphere system and understanding their interactions at different scales. Within the framework of IOP 3, a main focus was placed on the role of surface heterogeneities in atmospheric exchange, biogeochemistry and atmospheric chemistry. This study only concentrates on micrometeorological issues.

The experiment was conducted at the research site of the Bayreuth Centre of Ecological and Environmental Research (BayCEER) at the 'Waldstein' hillside in the 'Fichtelgebirge' mountains (Fig. 1a). The densely forested 'Fichtelgebirge' is a low mountain range that is located in north-eastern Bavaria, Germany; the 'Waldstein' is a mountainous ridge in the north-western part of the 'Fichtelgebirge'. The experimental site (50°8′N, 11°52′E, around 775 m a.s.l) lies in the upper catchment of the stream 'Lehstenbach' between the hilltops of 'Großer Waldstein' (879 m a.s.l) in the south-west and 'Bergkopf' (857 m a.s.l) in the north-east.

The measurements were carried out in a forest stand nearby the FLUXNET station 'Waldstein–Weidenbrunnen' (DE-Bay) and in a clear cutting, which is located south of the

Fig. 1 Location of the experimental site in the 'Fichtelgebirge' mountains (**a**, modified from Gerstberger et al. 2004) and an aerial picture showing the meterological towers/masts (M1–M4, M6–M8) within the patchy forest at 'Waldstein–Weidenbrunnen' (**b**, picture taken from Bayer. Landesvermessungsverwaltung, URL: http://www.geodaten.bayern.de/BayernViewer/index.cgi)

FLUXNET station (Fig. 1b). The clear cutting in its present dimensions can be attributed to a wind throw, which was caused by the storm Kyril on January 18, 2007 (Foken et al. 2012b). Furthermore, the northern border of the clear cutting was artificially straightened. The terrain of the measurement area is moderately sloped towards the south, and a description of the surrounding topography can be found in Thomas and Foken (2007b).

The forest is dominated by Norway spruce (*Picea abies*), whose stand age is approximately 60 years and the canopy height h is about 27 m. The leaf area index of the spruce trees is 4.8 $m^2 m^{-2}$ (Foken et al. 2012b) with the structure of the forest characterized by an open trunk space and a dense crown space. Most of the foliage is situated at a height between 0.5 and 0.9 z/h, where z is the measurement height and h is the canopy height (Staudt and Foken 2007). The understory covers about 60 to 80 % of the forest floor and its corresponding leaf area index is about 0.3 $m^2 m^{-2}$ (Gerstberger et al. 2004). Furthermore, young spruce trees are irregularly distributed within the sub-canopy layer, which are not included in the estimate of the leaf area index of the sub-canopy vegetation. The vegetation at the clearing is a mosaic of young spruce trees, herbaceous plants and dwarf shrubs. The heights of the plants range between 0.2 and 4.5 m, and vegetation cover as well as species composition are not homogeneous. Thus, it is difficult to determine a representative canopy height for the whole clearing. Within this study, the canopy height at the clear cutting is set to 0.9 m, which should be a reliable estimate for the vegetation around the location of turbulence measurements. For a detailed ecological description of the site, see Gerstberger et al. (2004). Reference data on climate, meteorology, vegetation structure and soil properties can be found in Staudt and Foken (2007).

2.2 Instrumentation

In order to quantify the spatial and temporal properties of coherent structures and their importance to turbulent transport across the forest edge, high-frequency turbulence mea-

surements were conducted along a transect perpendicular to the forest edge. Therefore, four towers, M1–M4, were set up along a forest-to-clearing transition (Fig. 1b). Meteorological towers M1 and M2 were situated within the forest, M3 was built up directly and at the forest edge, and mast M4 was erected at the clear cutting, 85 m south of M3. In order to retrieve information on the wind components (u, v and w) and sonic temperature (T_s), the masts were equipped with 3D sonic anemometers (USA-1, Metek GmbH; CSAT3 Campbell Scientific, Inc.). In most cases, these measurements were taken in conjunction with high-frequency optical gas analyzers (LI-7000, LI-7200, LI-7500, LI7500A, LI-COR Biosciences), which measure concentrations of carbon dioxide *(c)* and water vapour *(q)*. Within the forest (M2) and at the forest edge (M3) the measurement devices were set up at three levels: above the forest canopy ($z/h > 1.3$), around canopy top ($z/h \approx 1$) and at 2.25 m above the ground ($z/h \approx 0.1$). Furthermore, there is an additional meteorological tower in the forest (M1) where measurements were conducted only above the canopy ($z/h = 1.2$). Above the clearing (M4), measurements were taken at 2.25 m ($z/h \approx 6.1$) and at 5.5 m heights ($z/h \approx 2.5$).

In addition, three 3D sonic anemometers were installed at a height of 2.25 m in order to investigate horizontal coherent exchange around the forest edge. One was installed at the forest edge west of tower M3 (M6), another at the forest edge east of M3 (M7) and the third was mounted within the sub-canopy layer (M8). Consequently, the towers M4, M3 and M8 stand on a transect perpendicular to the forest edge and the towers M6, M3, and M7 on a transect along the forest edge.

All data were recorded at 20 Hz, except at M3 at 27 m height, where the measurement frequency was 10 Hz. The data from the main tower M1 should be taken with care, because the rather massive construction of M1 may strongly disturb the wind field. However, earlier measurements at 'Waldstein–Weidenbrunnen' (Thomas and Foken 2007b; Serafimovich et al. 2011b) have detected coherent structures with time scales ranging between 10 and 40s and it is assumed that the properties of such structures might be less affected. Table 1 shows an overview of the instrumentation, and for further information on experiment set-up, calibration parameters and data acquisition, see Serafimovich et al. (2011a).

2.3 Post-field Data Processing

Coherent motions appear as non-periodic ramps in scalar time series (Bergström and Högström 1989; Gao et al. 1989). To quantify their spatio-temporal characteristics, it is necessary to separate the individual coherent structures from the small-scale background turbulence (Thomas and Foken 2005), and in so doing, one should use automatic detection algorithms to ensure maximum objectivity of the results and to make different studies comparable. This section is mainly based on the works of Thomas and Foken (2005, 2007a,b), who advanced a concept of Collineau and Brunet (1993a,b). They developed a routine that is able to extract coherent structures from time series data and to determine time scales, length scales and flux contributions of coherent structures.

2.3.1 Data Preparation and Applied Corrections

The high-frequency measurements were stored into 30-min files, which were then processed individually. First, it was checked whether the data file had the expected number of values: if its size deviated by more than 5 % from the expected file size due to data loss, the 30-min file was not processed. Then, the measured gas concentrations of carbon dioxide and water vapour were corrected for density fluctuations (Webb et al. 1980), and the wind vector components were rotated by applying a sector-wise planar fit (Wilczak et al. 2001) in order

Table 1 Instrumentation of the meterological towers/masts (M1–M4, M6–M8) during EGER IOP 3 ($h_{forest} = 27$ m; $h_{clearcutting} = 0.9$ m) to conduct high-frequency measurements of the wind vector, sonic temperature T_s, carbon dioxide concentration c and water vapour concentration q

Tower	z (m)	z/h	Measured variables	Instrument	Period of measurement
M1	32	1.2	Wind vector, T_s	USA-1	June 13–July 26, 2011
			c, q	LI-7000	June 13–July 26, 2011
M2	36	1.3	Wind vector, T_s	USA-1	June 13–July 26, 2011
			c, q	LI-7500	June 13–July 26, 2011
	26	1.0	Wind vector, T_s	USA-1	June 18–July 26, 2011
	2.25	0.1	Wind vector, T_s	USA-1	June 18–July 26, 2011
M3	41	1.5	Wind vector, T_s	CSAT3	June 13–July 26, 2011
			c, q	LI-7500	June 13–July 26, 2011
	27	1.0	Wind vector, T_s	USA-1	June 13–July 05, 2011
			c, q	LI-7500	June 13–July 26, 2011
	2.25	0.1	Wind vector, T_s	CSAT3	June 20–July 26, 2011
			c, q	LI7500A	June 27–July 01, 2011
M4	5.5	6.1	Wind vector, T_s	CSAT3	June 13–July 26, 2011
			c, q	LI-7500	June 13–July 26, 2011
	2.25	2.5	Wind vector, T_s	CSAT3	June 13–July 26, 2011
			c, q	LI-7000	June 13–June 21, 2011
				LI-7200	June 21–July 26, 2011
M6	2.25	0.1	Wind vector, T_s	USA-1	June 20–July 26, 2011
M7	2.25	0.1	Wind vector, T_s	CSAT3	June 20–July 26, 2011
M8	2.25	0.1	Wind vector, T_s	USA-1	June 13–July 26, 2011

to remove the mean vertical wind within the 30-min files. Spikes within the time series were removed by a procedure according to Vickers and Mahrt (1997). Furthermore, in order to account for the time delay between the sonic anemometer and the gas analyzer, the time series were shifted using the time lag of the maximum of the cross-correlation. Afterwards, the 20 Hz data were averaged to 2 Hz in order to reduce computational time. This does not affect the results significantly because only high-frequency turbulence is removed. Furthermore, the time series are normalized by their mean value and, to prevent border effects, they are extended by adding zero values at both ends. The high-frequency fluctuations are removed by applying a low-pass filter. For this purpose, a discrete wavelet transformation with bio-orthogonal wavelets is run, which eliminates all fluctuations shorter than a critical event duration of 6.2 s (Thomas and Foken 2005).

2.3.2 Wavelet Analysis: Extraction of Coherent Structures

The wavelet transform (Grossmann and Morlet 1984; Kronland-Martinet et al. 1987; Grossmann et al. 1989) is a local transform that is able to resolve time series into the frequency domain and the time domain. It has been widely applied to atmospheric time series, (e.g. Collineau and Brunet 1993a; Feigenwinter and Vogt 2005; Thomas and Foken 2007a,b; Barthlott et al. 2007; Serafimovich et al. 2011b; Steiner et al. 2012). For an introduction into wavelet analysis of time series data, see Foufoula-Georgiou and Kumar (1994). The

description of the wavelet methodology applied here can be found in Thomas and Foken (2005).

After preparation of the 30-min files as mentioned above, a continuous wavelet transform was performed using the Morlet wavelet, from which the wavelet power spectrum was calculated. It displays the relative importance of different scales on the overall energy of the time series (Torrence and Compo 1998). Thus, if atmospheric transport is dominated by coherent eddies of a certain scale, the power spectrum should exhibit a distinct peak at that scale. Accordingly, the event duration of coherent structures (D_e) was inferred from the scale a_e of the first clearly expressed maximum in the wavelet spectrum, the peak frequency of the mother wavelet ($\omega^0_{\psi_{p,1,0}}$), and the time resolution of the time series (Δt, Thomas and Foken 2005),

$$D_e = \frac{a_e \Delta t \, \pi}{\omega^0_{\psi_{p,1,0}}}. \tag{2}$$

This first maximum in the spectrum is caused by the coherent structures developing in the mixing layer above the forest canopy, while additional structures due to the heterogeneity of the surrounding landscape cause additional peaks at larger scales in the wavelet variance spectrum (Zhang et al. 2007), which are not captured by the applied routine.

In order to extract individual coherent events, another wavelet transform was applied at the determined event duration. For this purpose the Mexican Hat wavelet is used, which is both localized in time and frequency. The zero-crossings method serves as a detection criterion for coherent structures (Collineau and Brunet 1993a), which proved to produce reliable results (Collineau and Brunet 1993b; Thomas and Foken 2005). However, the Mexican Hat wavelet has problems in separating coherent structures that immediately follow each other, and overestimates the number of coherent events during quiescent periods (Barthlott et al. 2007).

2.3.3 Determination of Properties of Coherent Structures

The event duration of coherent structures is given in Eq. 2, and the number of coherent structures N within a 30-min interval equals the number of zero-crossings in the Mexican Hat wavelet coefficients at the selected scale D_e. The mean temporal separation (T_x) between coherent structures can be calculated from the individual detection times ($t_{x,i}$) of the N coherent structures within the 30-min interval (Thomas and Foken 2007b), viz.

$$T_x = \frac{1}{N-1} \sum_{i=1}^{N-1} \left| t_{x,i} - t_{x,i+1} \right|. \tag{3}$$

The contribution of coherent structures was determined by a conditional sampling and averaging approach (Collineau and Brunet 1993b; Thomas and Foken 2007a). First, sub-samples of length $2\,D_e$ and centred on the detection times of individual coherent structures were collected from the time series. Then, a conditional average $\overline{\langle x' \rangle}$ of the fluctuating parts over all these sub-samples was calculated by applying the following operator,

$$\overline{\langle x' \rangle} = \frac{1}{D_e} \int_{-D_e}^{+D_e} \langle x'(t) \rangle \, dt. \tag{4}$$

The product of two averaged variables $\overline{\langle x' \rangle}\, \overline{\langle y' \rangle}$ yields that portion of the turbulent flux that is transported by coherent structures ($F_{cs,}$ Collineau and Brunet 1993b). It is explicitly not

the overall turbulent transport during the presence of coherent motions (Thomas and Foken 2007a), because the synchronous small-scale turbulent transport $\overline{\langle x'y' \rangle}$ is not captured via this technique. Coherent structures around high plant canopies comprise a sweep and an ejection. For simplicity, Thomas and Foken (2007a) assumed that the first half of the event is occupied by the ejection motion and the second half by the sweep. This order, i.e. that the ejection precedes the sweep, is independent of atmospheric conditions. Accordingly, the flux contribution of ejections (F_{ej}) and sweeps (F_{sw}) can be determined when the conditional averaging in Eq. 4 is restricted to the time intervals $[-D_e, 0]$ and $[0, +D_e]$, respectively.

2.3.4 Definition of Coupling Regimes

The following classification was developed for forests with a dense crown space and a rather open trunk space. The vertical heterogeneity of forests causes distinct regions of micrometeorological processes: the sub-canopy layer, the canopy layer and the atmosphere above the crown. Coherent structures can be regarded as single, large eddies that simultaneously exchange scalars and momentum between the forest and the atmosphere. According to Thomas and Foken (2007a), an observation layer at height z within the forest is defined to be coupled with the reference height z_{ref} above the canopy if the contributions of sweeps (F_{sw}) and ejections (F_{ej}) to sensible heat flux at height z are at least as large as their flux contributions at z_{ref}. To ensure that, the respective ratio of sensible heat fluxes carried by sweeps $F_{sw}(z_{ref})\, F_{sw}(z)^{-1}$ and ejections $F_{ej}(z_{ref})F_{ej}(z)^{-1}$ has to be smaller than the inverse slope a^{-1} of a linear regression of $\overline{w'T_S'}(z)$ versus $\overline{w'T_S'}(z_{ref})$:

$$\frac{F_{sw}\left(z_{ref}\right)}{F_{sw}(z)} < a^{-1} \wedge \frac{F_{ej}\left(z_{ref}\right)}{F_{ej}(z)} < a^{-1}. \tag{5}$$

Furthermore, a negative ratio $F_{sw}(z_{ref})\, F_{sw}(z)^{-1}$ or a negative ratio $F_{ej}(z_{ref})\, F_{ej}(z)^{-1}$ indicates opposite coherent flux directions and the two layers are also defined as being decoupled. On this basis, Thomas and Foken (2007a) defined five exchange regimes according to the number of forest layers that are coupled to the layer above the canopy, which serves as z_{ref}:

- *Wave motion* (Wa). The sub-canopy layer and forest canopy are decoupled from the layer above the canopy. Additionally, the flow above the canopy is dominated by linear gravity waves, which do not contribute to vertical fluxes (Cava et al. 2004).
- *Decoupled canopy* (Dc). In analogy to the Wa regime, both forest layers are decoupled from the atmosphere above.
- *Decoupled sub-canopy layer* (Ds). The canopy layer is coupled to the air above the canopy, but the sub-canopy layer is still decoupled.
- *Coupled sub-canopy layer by sweeps* (Cs). The canopy layer is coupled to the region above the canopy, but the sub-canopy layer is only coupled by the sweep motion, not by the ejection motion.
- *Fully coupled canopy* (C). At all canopy levels, both ejections and sweeps contribute to the exchange of energy and matter: all canopy layers are coupled to the air above the canopy.

A rigorous determination of the mass balance in a control volume requires that horizontal and vertical advection and flux divergences are taken into consideration (Stull 1988). In the case of advection, it is still not clear how to derive reliable advection estimates (Aubinet et al. 2010). In order to provide an alternative approach, Serafimovich et al. (2011b) have defined horizontal coupling by coherent structures. This approach is similar to the concept

of vertical coupling. The end of a transect serves as the reference point and instead of the vertical sensible heat flux, the horizontal sensible heat flux $\overline{u'T'_S}$ is used. On the assumption that coherent motions are the dominating turbulent transport mechanism in the sub-canopy layer, Serafimovich et al. (2011b) defined two different horizontal coupling regimes:

- *Horizontal decoupled state* (Dc$_h$). The ratios of $F_{sw}(z_{ref}) F_{sw}(z)^{-1}$ and $F_{ej}(z_{ref})$ $F_{ej}(z)^{-1}$ are negative or larger than a^{-1} (Eq. 5). Accordingly, there is no coupling from the reference site to the observation site.
- *Horizontal coupled state* (C$_h$). Coherent structures couple from the reference location to the observation location. The flux contribution of sweeps and ejections is larger at the observation site than at the reference site.

2.3.5 Quality Control of Processed Data

The analysis of long-term turbulence data requires a quality assessment and quality control (QA/QC) protocol (Thomas and Foken 2007b) to remove data collected under unfavourable conditions:

- Rejection of 30-min intervals when fog (visibility < 1000 m) or precipitation events are present. This was detected by a present weather detector (PWD-11, Vaisala). The subsequent 30-min interval was also removed in order to account for the drying of transducer heads and windows.
- Removal of periods when the vertical profiles of the mean horizontal velocity above the forest were disturbed. This is the case when $(dU/dz)_{z=h} \leq 0$, which is the requirement for preserving a plane mixing layer (Raupach et al. 1996).
- Exclusion of calm conditions with horizontal wind speeds at h below 0.3 m s^{-1} and rejection of free convection events and periods of strong stable stratification ($|h/L| > 1$, where L is the Obukhov length).

These criteria are site specific and based upon long-term measurement experience at the research site (Thomas and Foken 2007b). Altogether, 23 % of the 30-min periods between June 13 and July 26 2011 were rejected, mainly due to the presence of fog or precipitation (93 % of rejected data).

3 Results and Discussion

3.1 Time Scales of Coherent Structures

The size of coherent structures can be related to the height of the underlying vegetation (Paw et al. 1992; Finnigan 2000). The dominating time scale increases with the height of the roughness elements (Feigenwinter and Vogt 2005), and so, it is assumed that changes in surface properties between forest and clearing might affect the scales of coherent structures. The event duration of coherent structures (D_e) was determined from the wavelet variance spectrum using the Morlet wavelet, and the mean temporal separation between them (T_x) was calculated according to Eq. 3.

The time scales of coherent structures at the respective tops of towers M1–M4 exhibit no clear trend, i.e. except for w, there are not significantly shorter coherent events above the clear cutting (data not shown). This can be attributed to the small size of the clear cutting: the velocity and scalars cannot adapt to the new underlying surface. However, when focusing on
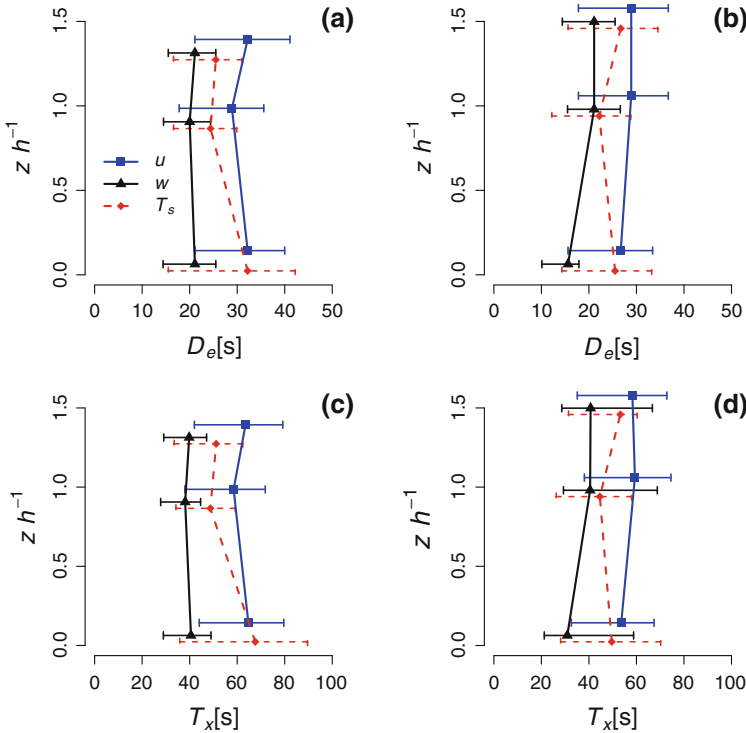
Fig. 2 Vertical profiles of event durations D_e (**a**, **b**) and streamwise distances T_x (**c**, **d**) of coherent structures within the forest at M2 (**a**, **c**), at the forest edge tower M3 (**b**, **d**) that were detected in the time series of the horizontal component wind component u, vertical wind component w and sonic temperature T_s; vertical axis shows measuring height z relative to canopy height h, *symbols* mark sample medians and *error bars* represent interquartile ranges

vertical profiles of coherent time scales (Fig. 2), a fundamental difference between the forest and the forest edge can be recognized. At M2 at canopy top (Fig. 2a), the event durations of coherent structures lie between 15 and 30 s, but in the sub-canopy layer, a clear increase of D_e and T_x in the time series of u and T_s can be recognized. Generally, the values are similar to the results of previous measurements at 'Waldstein–Weidenbrunnen', when Serafimovich et al. (2011b) also detected larger coherent structures in u and T_s mainly in the sub-canopy layer, with event durations ranging between 30 and 40 s. After the concept of Thomas and Foken (2007a), only the largest, most powerful coherent structures can penetrate through the forest crown and ensure that vertical exchange occurs. This is supported by the mean temporal separation of coherent structures (T_x), which is larger in the sub-canopy layer (Fig. 2c). An alternative explanation is delivered by Dupont et al. (2012), who state that structures within the forest are linked to above-canopy coherent motions by pressure diffusion and, due to this effect, they exhibit larger scales in the sub-canopy layer.

On the contrary, at the forest edge (Fig. 2b, d), the dense forest crown is missing. Accordingly, at M3, the time scales exhibit no clear trend between 41 m height and 2.25 m height. The smallest event durations and the highest arrival frequencies were expected at canopy top, due to the dense foliage below the measuring point (Baldocchi and Meyers 1988; Amiro 1990). But short event durations were also found at 2.25 m above the ground,
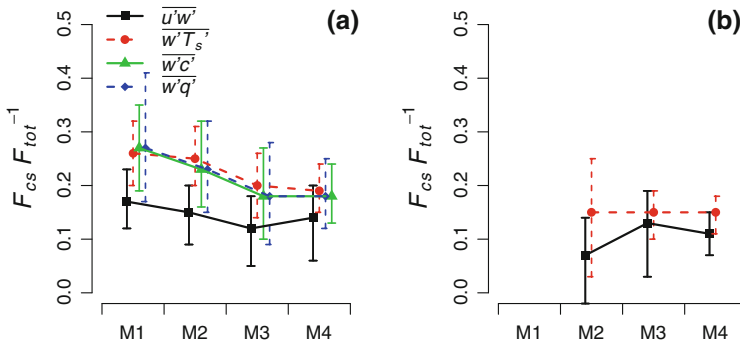
Fig. 3 The relative flux contribution of coherent structures F_{cs} to total fluxes F_{tot} of momentum $\overline{u'w'}$, buoyancy $\overline{w'T'_S}$, carbon dioxide $\overline{w'c'}$ and latent heat $\overline{w'q'}$ along the forest-to-clearing transect M1–M4, in (**a**), measurements were taken at tower tops (M1: 32 m, M2: 36 m, M3: 41 m, M4: 5.5 m); in (**b**), measurements were taken at 2.25 m height; *symbols* mark sample medians and *error bars* represent interquartile ranges

which indicates that there is no blocking of coherent structures from above by the crown layer.

Within the sub-canopy layer, the time scales of structures that are transporting scalars are almost identical to the scales of structures in the horizontal wind. At canopy top, time scales of scalars rather relate to the scales found in the vertical wind. Thomas and Foken (2007b) postulated that coherent structures transport scalars mainly laterally, because the scales of scalar structures resemble structures that transport momentum. However, at least for the measurements around canopy top, this relation does not hold true. There, the time scales found in scalar time series are similar to time scales found in w. Meteorological towers within forests are usually located in small gaps between the trees, where vertical exchange between forest and atmosphere can take place, but lateral transport is prevented by the foliage of the surrounding trees. Thus, around the crown, coherent structures transport scalar entities mainly vertically, whereas they propagate horizontally in the sub-canopy layer and above the canopy.

3.2 Coherent Flux Contribution

In this section, the relative importance of coherent structures to the total turbulent fluxes (F_{tot}) between forest, forest edge and clear cutting will be compared. Coherent fluxes (F_{cs}) were determined by a conditional sampling approach, as described in Sect. 2.3.3.

Above the forest stand, the flux contribution of coherent structures $F_{cs} F_{tot}^{-1}$ continuously decreases when moving from forest to clear cutting (Fig. 3a). Values of $F_{cs} F_{tot}^{-1}$ of $\overline{w'T'_S}$, $\overline{w'q'}$ and $\overline{w'c'}$ lie between 24 and 29 % above the forest canopy and around 19 % above the clear cutting and the forest edge. Coherent structures generally contribute less to momentum flux, which is confirmed by the results of Barthlott et al. (2007), Thomas and Foken (2007a) and Serafimovich et al. (2011b). Values of $F_{cs} F_{tot}^{-1}$ above the forest are similar to those that Thomas and Foken (2007a) and Serafimovich et al. (2011b) found at 'Waldstein–Weidenbrunnen'. Furthermore, they are quite in accordance with the results of Collineau and Brunet (1993b), who measured larger flux contributions (26 % for momentum flux, 40 % for sensible heat flux), but above a regularly planted pine forest. Steiner et al. (2012), though, determined flux contributions up to 50 % above a mixed deciduous forest, as well as Barthlott et al. (2007) above open field. These higher values can be explained by a methodological difference: Barthlott et al. (2007) and Steiner et al. (2012) apply the concept

of Lu and Fitzjarrald (1994) who state that, during the presence of a coherent structure, the total flux should be defined to be a coherent flux. In contrast, this study follows the ideas of Collineau and Brunet (1993b) and Thomas and Foken (2007a), who consider a coherent structure to be a single entity with one distinct temporal scale that is superimposed on high-frequency, stochastic turbulence.

Coherent structures contribute less to vertical exchange at the forest-to-clearing transition and above the clear cutting (12 % for momentum flux and 17–19 % for scalar fluxes) than above the forest. With respect to the forest edge, one could claim that the larger distance from the forest canopy at M3 might be the reason for smaller coherent flux contributions. Coherent structures generally contribute most near the forest crown, where most of the foliage is concentrated (Serafimovich et al. 2011b). However, it is possible that the captured structures are not the dominant transport mechanism at the forest edge. As described in Sect. 2.3.2, only one single scale of coherent structures was captured, presumably those structures that evolve out of Kelvin–Helmholtz instabilities at forest top. It is not surprising that coherent structures caused by the wind shear at the top of the forest canopy (Raupach et al. 1996) contribute less to vertical exchange above the forest edge, as these motions are supposed to weaken when their formation mechanism is missing. Dupont and Brunet (2009) argue that coherent structures need a distance of $9h$ behind a leading forest edge until they have completely grown. This is in accordance with a large-eddy simulation study of Huang et al. (2011), who found that typical coherent motions which relate to the underlying surface properties are weakened at the surface transition. This does not necessarily mean that the flux at the forest edge is less coherent. Secondary circulations may dominate coherent transport at the forest edge (Zhang et al. 2007).

At 2.25 m height (Fig. 3b), coherent structures generally contribute less to turbulent fluxes than at the top of the respective measurement tower. The extremely low flux contribution of coherent structures at the bottom of M2 (6 % for $\overline{u'w'}$ and 15 % for $\overline{w'T'_S}$) stands in contrast to the results of Thomas and Foken (2007a), who claimed that coherent structures in the sub-canopy layer should have flux contributions larger than 50 %. However, Serafimovich et al. (2011b) also detected a comparable decrease of $F_{cs} F_{tot}^{-1}$ in the sub-canopy layer and Gao et al. (1989) showed that coherent structures weaken below the foliage of a deciduous forest dominated by maple and aspen. Vertical profiles (Fig. 4a, d) show that within the forest in contrast to the forest edge, coherent structures contribute most to turbulent fluxes at canopy top due to the immediate vicinity of the forest crown. This was also found by Collineau and Brunet (1993b) and Serafimovich et al. (2011b). At all measurement heights at the forest edge, coherent structures contribute less than within the forest, which supports the statement that structures originating from the mixing layer are not the dominant exchange mechanism at the forest edge.

When focusing on the contributions of sweeps and ejections at the forest edge (Fig. 4b, c), it can be stated that sweeps contribute more around the canopy top. There are numerous studies that confirm that sweeps dominate in the middle and upper canopy layers (e.g. Shaw et al. 1983; Bergström and Högström 1989; Maitani and Shaw 1990). Poggi et al. (2004) and Katul et al. (2006) claim that this is an inherent property of dense plant canopies. In the roughness sublayer above the forest, the ejection motion is stronger than at the canopy top, which is in accordance with previous studies (Bergström and Högström 1989; Maitani and Shaw 1990; Poggi et al. 2004; Katul et al. 2006; Serafimovich et al. 2011b).

At the forest edge, (Fig. 4e, f) there is no clear vertical trend, presumably because the forest nearby has only a minor impact on coherent exchange. However, sweeps dominate
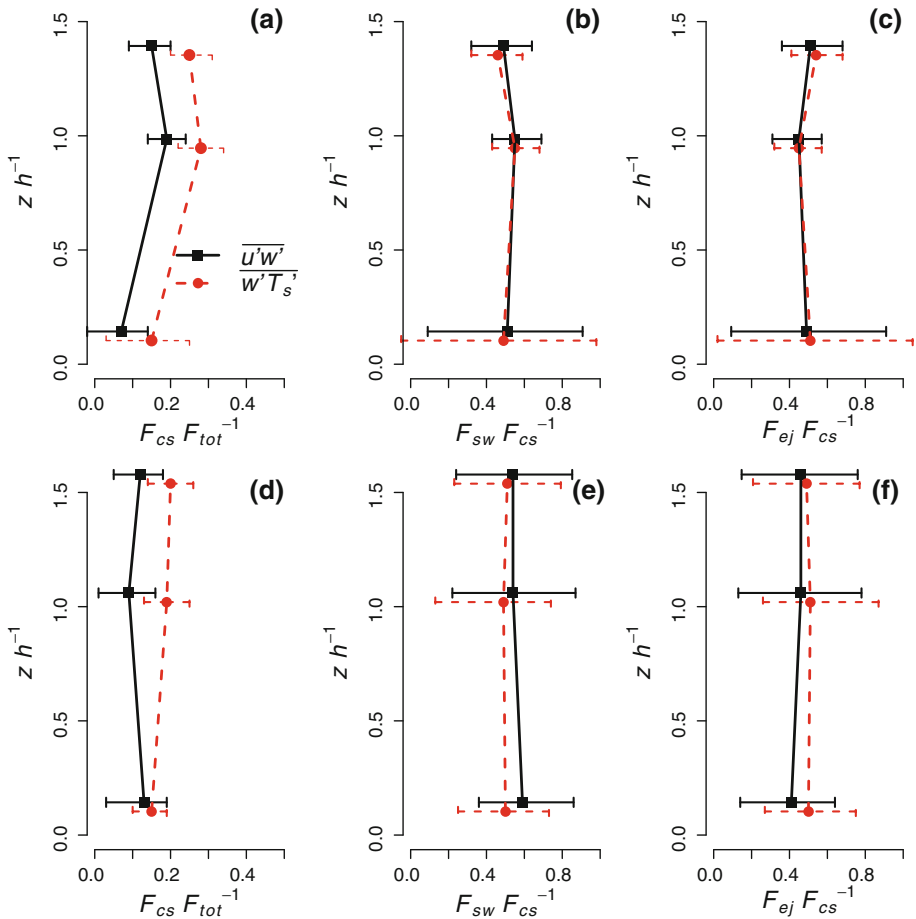
Fig. 4 Vertical profiles of the relative flux contribution of coherent structures $F_{cs} F_{tot}^{-1}$ (**a, d**), contributions of sweeps F_{sw} (**b, e**) and ejections F_{ej} (**c, f**) to coherent transport F_{cs} of momentum flux $\overline{u'w'}$ and buoyancy flux $\overline{w'T_S'}$ within the forest at M2 (**a–c**), at the forest edge tower M3 (**d–f**); *vertical axis* shows measuring height z relative to canopy height h, *symbols* mark sample medians and *error bars* represent interquartile ranges

the coherent flux of momentum at all measurement heights, probably due to the main wind direction (west, see Sect. 3.5).

3.3 Vertical Coupling Regimes

As coherent structures are supposed to be the main reason for the exchange of scalars and momentum between the forest and the atmosphere, vertical exchange regimes (Thomas and Foken 2007a) are defined on the basis of vertical profiles of coherent flux contributions (Sect. 2.3.4). In Sect. 3.1, it was argued that coherent structures can easily propagate vertically at the forest edge, whereas, within the forest, the air is temporary decoupled from the overlying atmosphere. However, at the forest edge, the flux contributions of coherent structures (Sect. 3.2) are lower than within the forest suggesting that coherent motions with time scales between 10 and 40 s may not ensure better coupling at the forest edge. Therefore,
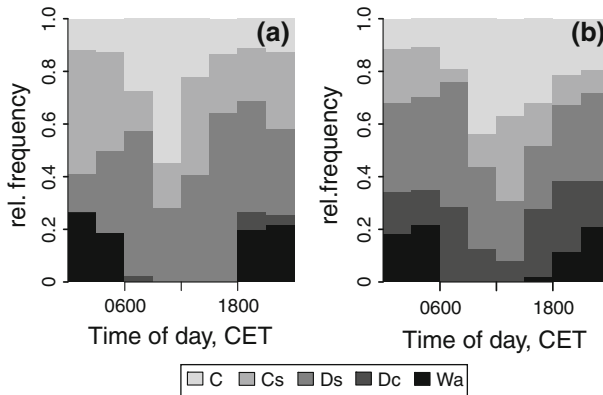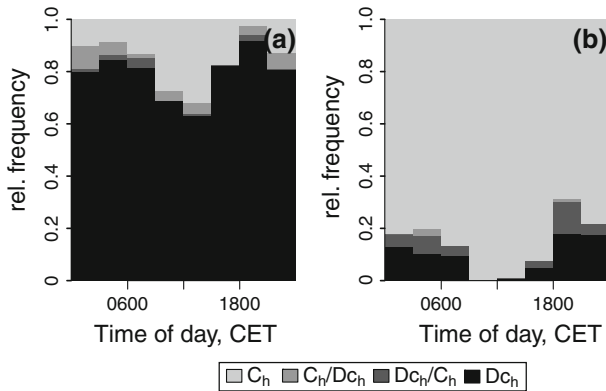
Fig. 5 Relative frequency of vertical coupling regimes as a function of time of day, both within the forest at M2 (**a**) and at the forest edge tower M3 (**b**); abbreviations of coupling regimes are according to Sect. 2.3.4; due to malfunction of some devices, only the data between June 21, 2011 and July 02, 2011 were used

the vertical coupling regimes at the forest edge (M3) and in the forest (M2) are compared (Fig. 5). At the forest edge tower M3 at 27 m height, data are only available up to July 2, 2011, so that the vertical coupling regimes were calculated only for the time period from June 13 to July 2, 2011, when all measurement devices were working.

Generally, at both sites, there is a clear daily cycle. Decoupled situations (Wa and Dc) mostly occur at night (1800-0600 h), but only when the friction velocity is low ($< 0.5\mathrm{m\,s}^{-1}$). Within the forest, decoupled situations are mainly associated with gravity waves (Wa regime) that occur in situations with very stable stratification (Cava et al. 2004) and low wind shear (Goeckede et al. 2007). Nevertheless, the forest is not always decoupled from the overlying atmosphere at night: from time to time, even a complete coupling (regimes C and Cs) of the forest by coherent structures occurs. However, C and Cs regimes are more frequent during the daytime, when the canopy layer of the forest (M2) is permanently coupled to the overlying atmosphere (regimes C, Cs and Ds). This daily cycle is typical of the coniferous forest at 'Waldstein/Weidenbrunnen', which has a dense crown and an open trunk space (Thomas and Foken 2007a; Serafimovich et al. 2011b; Foken et al. 2012b). In contrast, Steiner et al. (2012) did not find a diurnal cycle of the coupling regimes, but they determined the vertical coupling only with measurements at canopy top and above the canopy, and so they could not detect whether the sub-canopy layer is decoupled from the overlying layers. Moreover, they defined coupling on the basis of total fluxes and not on the basis of coherent fluxes.

In the morning hours and in the late afternoon, there are considerable differences between the coupling regimes in the forest (Fig. 5a) and at the forest edge (Fig. 5b). In the morning hours, the forest site is already well coupled to the overlying roughness sublayer, but the forest edge site is not. The atmospheric stratification (z/L) correlates with the vertical coupling regimes (Goeckede et al. 2007) and might be responsible for the observed differences. The clear cutting cools more than the adjacent forest site during the night and the resulting stable stratification prevents coherent structures that can propagate vertically in the morning hours. During the afternoon, the forest sub-canopy layer is mainly decoupled from the overlying atmosphere, i.e. the Ds regime dominates at M2 from 1500 to 1800h. This observation was also made during earlier IOPs of the EGER project (Foken et al. 2012b), when decoupling was caused by an oasis effect (Stull 1988; Foken 2008a): in the late afternoon, the latent heat flux is larger than the net radiation because the trees maintain very high evaporation rates;

Fig. 6 Relative frequency of the horizontal coupling regimes (C_h: complete coupling, C_h/Dc_h: first two towers coupled but second and third tower decoupled, Dc_h/C_h: first two towers decoupled but second and third tower coupled, Dc_h: complete decoupling) as a function of time of day, both along the transect M8–M3–M4 perpendicular to the forest edge (**a**) and along the transect M6–M3–M7 along the forest edge tower M3 (**b**); the respective measurements were taken at 2.25 m above ground; data from the whole measurement period (June 13, 2011–July 26, 2011) were used

consequently, the sensible heat flux above the forest crown becomes negative, stable stratification develops, and finally, the sub-canopy layer becomes decoupled from the atmosphere above. At the forest edge, stable stratification does not occur until sunset because the clear cutting is too dry to produce a considerable oasis effect, and so there is improved vertical coupling at the forest edge in the late afternoon.

Finally, it should be mentioned that, at the forest edge, the vertical coupling is not stronger than within the forest, which is in accordance with the findings of Sect. 3.2. The relative frequency of coupled situations (C and Cs) at the forest edge (36.4 %) is lower than within the forest (48.9 %). Moreover, at the forest edge, there is a large number of Dc situations, an exchange regime that was rarely detected within the forest. Thus, organized structures that evolve from the mixing layer above the forest are not the dominating vertical coupling mechanism at the forest edge.

3.4 Horizontal Coupling Regimes

Horizontal coupling by coherent structures was analyzed along two different transects: one along the forest edge (towers M6, M3, M7) and one perpendicular to the forest edge (towers M8, M3, M4). Following Sect. 2.3.4, two towers are defined to be coupled or decoupled on the basis of coherent flux contributions to horizontal turbulent fluxes. Because an array of three towers along each direction was analyzed, the following horizontal exchange regimes were defined: all measurement points are coupled (C_h), all points are decoupled (Dc_h), the first pair is coupled but the second is not (C_h/Dc_h) and vice versa (Dc_h/C_h).

Generally, there is a better horizontal coupling by coherent structures along the forest edge: the towers M6, M3 and M7 were coupled (C_h) during 86 % of all 30-min periods, but M8, M3 and M4 only during 16 %. Because the horizontal coupling is mainly controlled by the wind direction and the vegetation structure (Serafimovich et al. 2011b; Foken et al. 2012b), there are two main reasons for this remarkable difference: (i) there are apparently less obstacles (trees) along the forest edge, which facilitates the propagation of coherent structures, and (ii) the transect M6–M3–M7 is approximately in the same direction as the

Table 2 Probability (%) of horizontal exchange regimes (abbreviations according to Fig. 6) perpendicular to the forest edge (M8–M3–M4) and along the forest edge (M6–M3–M7) as a function of synchronous vertical coupling regimes (abbreviations according to Sect. 2.3.4) at the forest edge tower M3

Vertical coupling at M3	Associated horizontal regime	Proportion perpendicular to forest edge (M8–M3–M4, %)	Proportion along forest edge (M6–M3–M7, %)
Wa/Dc	Dc_h	75	14
	Dc_h/C_h and C_h/Dc_h	13	12
	C_h	13	74
Ds	Dc_h	74	9
	Dc_h/C_h and C_h/Dc_h	8	3
	C_h	17	88
C/Cs	Dc_h	71	6
	Dc_h/C_h and C_h/Dc_h	7	2
	C_h	22	93

mean flow. At the site, westerly winds dominate due to the channelling of the flow by the hills "Bergkopf" and "Großer Waldstein".

Furthermore, a weak daily cycle can be recognized along both transects with a larger fraction of horizontal coupled situations during the daytime and decoupling during the night (Fig. 6). A weak relationship between the vertical coupling regimes at tower M3 and the horizontal coupling along M6–M3–M7 and M8–M3–M4 towers can be found (Table 2). When C/Cs regimes prevail in the vertical direction, there is a larger probability that good coupling (C_h) occurs in the horizontal direction.

Because the wind direction plays an important role for the horizontal coupling, we tested whether it is the reason for the rare decoupled situations along the forest edge and the coupled situations perpendicular to the forest edge (data not shown). For the transect M6–M3–M7, northerly wind directions prevailed during those nighttime samples with a Dc_h regime. So, we suppose that the decoupling along the forest edge during night is associated with drainage flows that follow the terrain that is inclined to the south. However, this drainage flow is not accompanied by coupling along the transect perpendicular to the forest edge (M8–M3–M4). This flow should be regarded as a quasi-laminar mass flow associated with insufficient mixing (Aubinet et al. 2003; Staebler and Fitzjarrald 2004) that might ensure the transport of air constituents out of the forest. During the daytime, no influence of the wind direction on horizontal coupling along transects M6–M3–M7 and M8–M3–M4 can be identified.

3.5 Secondary circulation above the clear cutting

As stated in the previous sections, coherent structures with time scales between 10 and 40s are not the relevant vertical transport mechanism at the forest edge. However, there are some indications that there is a secondary circulation above the clear cutting that might be responsible for significant vertical exchange.

In the immediate vicinity of the roughness heterogeneity, the shape of coherent structures changes during the day, and the flux contributions of sweeps and ejections follow a distinct daily pattern (Fig. 7): whereas sweeps dominate during the night, ejections contribute more to coherent exchange during the daytime. This effect was only discovered at the forest edge
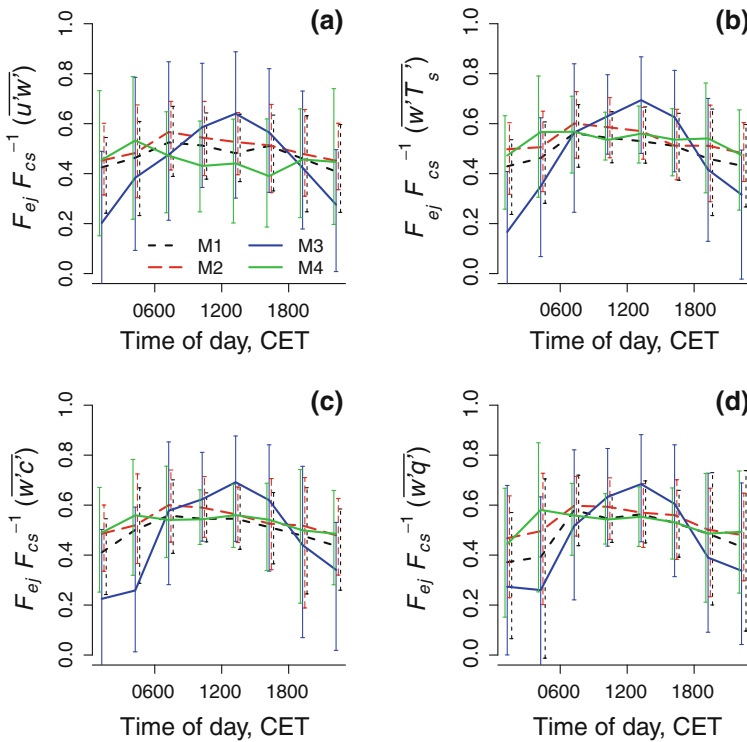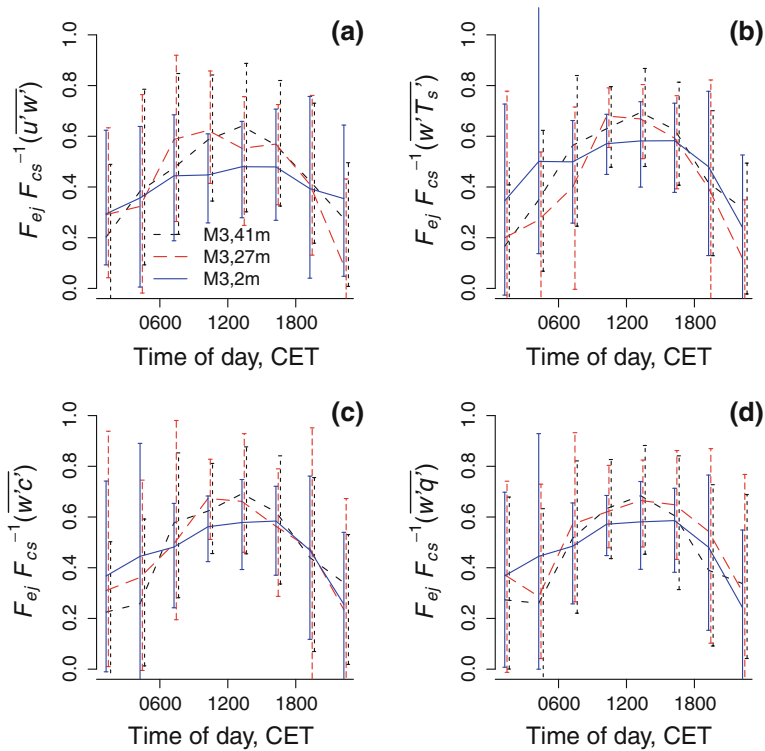
Fig. 7 Daily cycle of the ejection contribution to coherent transport $F_{ej} F_{cs}^{-1}$ of momentum flux $\overline{u'w'}$ (**a**), buoyancy flux $\overline{w'T'_s}$ (**b**), flux of carbon dioxide $\overline{w'c'}$ (**c**) and latent heat flux $\overline{w'q'}$ (**d**) at the tops of measurement towers M1-M4 (M1: 32 m, M2: 36 m, M3: 41 m, M4: 5.5 m); for the purpose of clarity, 3-h averages were calculated from medians of 30-min data; *error bars* represent interquartile ranges

tower M3, but not above the forest (towers M1, M2) and the clear cutting (tower M4). This effect might be caused by secondary circulations that have even longer time scales than the coherent eddies from the mixing layer at the canopy top.

A secondary circulation is defined as an "organized flow superimposed on a larger-scale mean circulation" Glickman (2000). In the framework of this study, and according to Foken (2008b), secondary circulations are motions that are caused by surface heterogeneities and that are superimposed on the mean flow. The 'Waldstein/Weidenbrunnen' experimental site exhibits heterogeneities in both topography and forest structure. Presumably, there might be a secondary circulation above the 'Köhlerloh' clear cutting: during the daytime, the clear cutting heats up, which triggers thermal updrafts. The adjacent forest edge is the region where such a stationary circulation enhances turbulent fluxes (Klaassen et al. 2002; Leclerc et al. 2003). As a result, this circulation modulates the coherent structures at the edge: during the daytime, the upward-directed ejections dominate whereas during at night, the strong cooling of the clear cutting induces strong sweeps at the forest edge.

It is still not clear whether secondary circulations reach the ground, because they cannot be captured with typical eddy-covariance measurements near the surface (Foken 2008b). When focusing on the daily cycle of the ejection contributions at the forest edge (Fig. 8), it can be seen that, at all heights, ejections contribute more to the coherent flux during the daytime. This daily pattern is weakened at 2.25 m with respect to the momentum flux, but not for

Fig. 8 Daily cycle of the ejection contribution to coherent transport $F_{ej}F_{cs}^{-1}$ of momentum flux $\overline{u'w'}$ (**a**), buoyancy flux $\overline{w'T_S'}$ (**b**), flux of carbon dioxide $\overline{w'c'}$ (**c**) and latent heat flux $\overline{w'q'}$ (**d**) at the forest edge tower M3 at different measuring heights (41 m, 27 m, 2.25 m); for the purpose of clarity, 3-h averages were calculated from medians of 30-min data; *error bars* represent interquartile ranges; please note that at 27 m height, measurements are available only up to July 03, 2011, whereas for the other two heights, data are available up to July 26, 2011

the scalar fluxes. Thus, the secondary circulation above the clear cutting influences coherent structures down to the ground. Because such an impact on the ejection-sweep cycle was not identified at 5.5 m above the clear cutting (Fig. 7), it can be concluded that this effect only takes place in the vicinity of the forest edge.

It could be argued that the daily cycle of the ejections and sweeps is the result of a systematic flow distortion by the forest edge, because this represents a huge obstacle for the wind field and might modulate the shape of coherent structures as well as their importance for turbulent fluxes. Therefore, the data from the top of tower M3 were divided into three wind sectors (Fig. 9a). There are two sectors for the clear cutting, because an earlier study at the research site (Thomas and Foken 2007b) showed that the coherent structures from the south-eastern directions largely differ from those of the other sectors. However, in this study, no considerable differences were found between south-eastern and western wind directions and no distinct influence of the wind direction on the total coherent flux was detected. However, the relative magnitudes of sweeps and ejections depend on wind direction (Fig. 9b): when the flow impacts upon the leading forest edge from the southern and western directions, the sweep motions become slightly stronger. This effect was also found by Huang et al. (2011), who simulated coherent structures between a clear cutting and an artificial forest
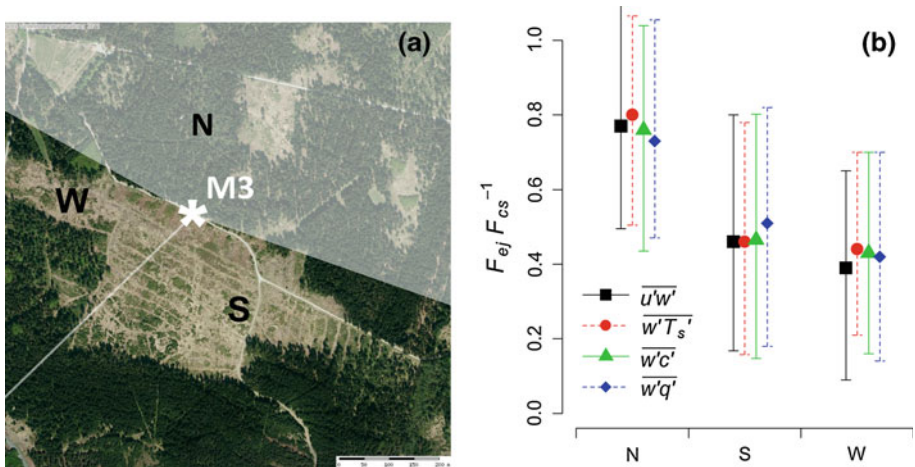
Fig. 9 Selected wind sectors (N: north, W: west, S: south) at forest edge tower M3 (**a**, source: see Fig. 1b) and respective contribution of ejections to coherent transport $F_{ej} F_{cs}^{-1}$ of momentum $\overline{u'w'}$, buoyancy $\overline{w'T'_S}$, carbon dioxide flux $\overline{w'c'}$ and latent heat flux $\overline{w'q'}$ for the different wind sectors at 41 m height (**b**); *symbols* mark sample medians and *error bars* represent interquartile ranges

block. These sweeps appear just behind the leading edge of the forest, because this effect was not detected at the M2 tower. When the wind direction is from the forest to the clear cutting, very strong ejections can be detected above the forest edge. One explanation might be that, at M3, the measurements were taken at the largest distance from the forest canopy: the devices were installed well above the forest canopy ($z/h = 1.52$), where ejections usually dominate coherent exchange (Bergström and Högström 1989; Maitani and Shaw 1990; Poggi et al. 2004; Katul et al. 2006; Serafimovich et al. 2011b). However, such strong ejection contributions above forest canopies cannot be found in the literature, and consequently, the ejections might be rather an effect of the trailing edge of the forest.

In order to clarify whether the daily pattern of ejections and sweeps is caused by the wind direction relative to the forest edge, we tested whether certain wind sectors (Fig. 9a) dominate during the day or during night. However, no dependence of the wind direction on the time of day was found. Consequently, the dominance of ejections the during day and sweeps at night cannot be explained by the flow distortion due to the forest edge, and so it is probably caused by a secondary circulation above the clear cutting.

4 Conclusions

The aim of this study was to identify the impact of surface characteristics on the properties of coherent structures at a forest, a forest edge and an adjacent clear cutting by using a wavelet technique. With respect to time scales, no considerable differences above the forest canopy and above the clear cutting were detected. But longer time scales in the forest sub-canopy layer were found, indicating that not all coherent structures can penetrate through the canopy. Such an effect was not identified at the forest edge, suggesting a better vertical propagation of structures there. However, coherent structures with time scales between 10 and 40 s contribute less above the forest edge and the clear cutting than above the forest canopy. It is assumed that these structures develop in the mixing layer above the forest and vanish above the clear cutting and accordingly, they contribute less to turbulent fluxes there.

Furthermore, insights were given into the horizontal and vertical coupling (Thomas and Foken 2007b; Serafimovich et al. 2011b) by coherent structures around a forest edge. With respect to horizontal coupling by coherent structures, there is considerable better coupling along the forest edge than perpendicular to it, mainly because the forest edge is approximately aligned with the mean wind direction. Superimposed on this general feature, coherent structures couple better horizontally during daytime, which is independent of wind direction or transect orientation. Better coupling during the day was also found in the vertical direction, both within the forest and at the forest edge. Furthermore, the vertical coupling in the forest is stronger than at the forest edge, which is in accordance with the measured flux contributions.

However, there are some indications that there is another relevant transport mechanism: secondary circulations above the clear cutting. These circulations modify the shape of coherent structures, yet only directly at the forest edge: strong ejection motions cause a systematic outflow of air during the daytime, whereas during the night strong sweep motions transport fresh air from the overlying atmosphere to the surface. Because this observation cannot be explained by differences in prevailing wind directions during the daytime and at night, it is argued that quasi-stationary circulations due to surface heterogeneities have a considerable effect on the exchange process in complex landscapes.

References

Amiro BD (1990) Comparison of turbulence statistics within three boreal forest canopies. Boundary-Layer Meteorol 51:99–121

Antonia RA (1981) Conditional sampling in turbulence measurement. Annu Rev Fluid Mech 13:131–156

Aubinet M, Feigenwinter C, Heinesch B, Bernhofer C, Canepa E, Lindroth A, Montagnani L, Rebmann C, Sedlak P, Van Gorsel E (2010) Direct advection measurements do not help to solve the night-time CO_2 closure problem: evidence from three different forests. Agric For Meteorol 150:655–664

Aubinet M, Grelle A, Ibrom A, Rannik Ü, Moncrieff J, Foken T, Kowalski AS, Martin PH, Berbigier P, Bernhofer C, Clement R, Elbers J, Granier A, Grünwald T, Morgenstern K, Pilegaard K, Rebmann C, Snijders W, Valentini R, Vesala T (2000) Estimates of the annual net carbon and water exchange of forests: the EUROFLUX methodology. Adv Ecolog Res 30:113–175

Aubinet M, Heinesch B, Yernaux M (2003) Horizontal and vertical CO_2 advection in a sloping forest. Boundary-Layer Meteorol 108:397–417

Baldocchi DD, Meyers TP (1988) A spectral and lag-correlation analysis of turbulence in a deciduous forest canopy. Boundary-Layer Meteorol 45:31–58

Barthlott C, Drobinski P, Fesquet C, Dubos T, Pietras C (2007) Long-term study of coherent structures in the atmospheric surface layer. Boundary-Layer Meteorol 125:1–24

Bergström H, Högström U (1989) Turbulent exchange above a pine forest II. Organized structures. Boundary-Layer Meteorol 49:231–263

Cantwell BJ (1981) Organized motion in turbulent flow. Annu Rev Fluid Mech 13:457–515

Cassiani M, Katul GG, Albertson JD (2008) The effects of canopy leaf area index on airflow across forest edges: large-eddy simulation and analytical results. Boundary-Layer Meteorol 126:433–460

Cava D, Giostra U, Siqueira M, Katul G (2004) Organised motion and radiative perturbations in the nocturnal canopy sublayer above an even-aged pine forest. Boundary-Layer Meteorol 112:129–157

Cellier P, Brunet Y (1992) Flux-gradient relationships above tall plant canopies. Agric For Meteorol 58:93–117

Collineau S, Brunet Y (1993a) Detection of turbulent coherent motions in a forest canopy part I: wavelet analysis. Boundary-Layer Meteorol 65:357–379

Collineau S, Brunet Y (1993b) Detection of turbulent coherent motions in a forest canopy part II: time-scales and conditional averages. Boundary-Layer Meteorol 66:49–73

Denmead OT, Bradley EF (1985) Flux-gradient relationships in a forest canopy. In: Hutchinson BA, Hicks BB (eds) The forest-atmosphere interaction. D. Reidel Publishing Company, Dordrecht, pp 421–442

Denmead OT, Bradley EF (1987) On scalar transport in plant canopies. Irrig Sci 8:131–149

Detto M, Katul GG, Siqueira M, Juang JY, Stoy P (2008) The structure of turbulence near a tall forest edge: the backward-facing step flow analogy revisted. Ecol Appl 18:1420–1435

Dupont S, Brunet Y (2009) Coherent structures in canopy edge flow: a large-eddy simulation study. J Fluid Mech 630:93–128

Dupont S, Irvine M, Bonnefond JM, Lamaud E, Brunet Y (2012) Turbulent structures in a pine forest with a deep and sparse trunk space: stand and edge regions. Boundary-Layer Meteorol 143:309–336

Fazu C, Schwerdtfeger P (1989) Flux-gradient relationships for momentum and heat over a rough natural surface. Q J R Meteorol Soc 115:335–352

Feigenwinter C, Vogt R (2005) Detection and analysis of coherent structures in urban turbulence. Theor Appl Climatol 81:219–230

Finnigan J (1979) Turbulence in waving wheat. Boundary-Layer Meteorol 16:213–236

Finnigan J (2000) Turbulence in plant canopies. Annu Rev Fluid Mech 32:519–571

Foken T (2008a) Micrometeorology. Springer, Heidelberg, p 308

Foken T (2008b) The energy balance closure problem: an overview. Ecol Appl 18:1351–1367

Foken T, Leuning R, Oncley SR, Mauder M, Aubinet M (2012a) Corrections and data quality control. In: Aubinet M, Vesala T, Papale D (eds) Eddy covariance: a practical guide to measurement and data analysis. Springer, Dordrecht, pp 85–131

Foken T, Meixner FX, Falge E, Zetzsch C, Serafimovich A, Bargsten A, Behrendt T, Biermann T, Breuninger C, Dix S, Gerken T, Hunner M, Lehmann-Pape L, Hens K, Jocher G, Kesselmeier J, Lüers J, Mayer J-C, Moravek A, Plake D, Riederer M, Rütz F, Scheibe M, Siebicke L, Sörgel M, Staudt K, Trebs I, Tsokankunku A, Welling M, Wolff V, Zhu Z (2012b) Coupling processes and exchange of energy and reactive and non-reactive trace gases at a forest site: results of the EGER experiment. Atmos Chem Phys 12:1923–1950

Foufoula-Georgiou E, Kumar P (1994) Wavelet analysis in geophysics: an introduction. In: Foufoula-Georgiou E, Kumar P (eds) Wavelets in geophysics. Academic Press, San Diego, pp 1–44

Gao W, Shaw RH, Paw UKT (1989) Observation of organized structure in turbulent flow within and above a forest canopy. Boundary-Layer Meteorol 47:349–377

Garratt JR (1978) Flux profile relations above tall vegetation. Q J R Meteorol Soc 104:199–211

Garratt JR (1980) Surface influence upon vertical profiles in the atmospheric near-surface layer. Q J R Meteorol Soc 106:803–819

Gerstberger P, Foken T, Kalbitz K (2004) The Lehstenbach and Steinkreuz catchments in NE Bavaria, Germany. In: Matzner E (ed) Biogeochemistry of forested catchments in a changing environment: a german case study. Springer, Berlin, pp 15–41

Glickman TS (ed) (2000) Glossary of meteorology, 2nd edn. American Meteorological Society, Boston, p 855

Goeckede M, Thomas C, Markkanen T, Mauder M, Ruppert J, Foken T (2007) Sensitivity of Lagrangian stochastic footprints to turbulence statistics. Tellus B 59:577–586

Grossmann A, Kronland-Martinet R, Morlet J (1989) Reading and understanding continous wavelet transforms. In: Combes JM, Grossmann A, Tchamitchian P (eds) Wavelets: time-frequency methods and phase space. Springer, New York, pp 2–20

Grossmann A, Morlet J (1984) Decomposition of hardy functions into square integrable wavelets of constant shape. SIAM J Math Anal 15:723–736

Harman I, Finnigan J (2007) A simple unified theory for flow in the canopy and roughness sublayer. Boundary-Layer Meteorol 123:339–363

Harman I, Finnigan J (2008) Scalar concentration profiles in the canopy and roughness sublayer. Boundary-Layer Meteorol 129:323–351

Holmes P, Lumley JL, Berkooz G (1996) Turbulence, coherent structures, dynamical systems and symmetry. Cambridge University Press, New York, p 420

Huang J, Cassiani M, Albertson J (2011) Coherent turbulent structures across a vegetation discontinuity. Boundary-Layer Meteorol 140:1–22

Inagaki A, Castillo M, Yamashita Y, Kanda M, Takimoto H (2012) Large-eddy simulation of coherent flow structures within a cubical canopy. Boundary-Layer Meteorol 142:207–222

Katul G, Poggi D, Cava D, Finnigan J (2006) The relative importance of ejections and sweeps to momentum transfer in the atmospheric boundary layer. Boundary-Layer Meteorol 120:367–375

Klaassen W, Breugel PB, Moors EJ, Nieveen JP (2002) Increased heat fluxes near a forest edge. Theor Appl Climatol 72:231–243

Kline SJ, Reynolds WC, Schraub FA, Runstadler PW (1967) The structure of turbulent boundary layers. J Fluid Mech 30:741–773

Kronland-Martinet R, Morlet J, Grossmann A (1987) Analysis of sound patterns through wavelet transforms. Int J Pattern Recog 1:273–302

Leclerc MY, Karipot A, Prabha T, Allwine G, Lamb B, Gholz HL (2003) Impact of non-local advection on flux footprints over a tall forest canopy: a tracer flux experiment. Agric For Meteorol 115:19–30

Lu CH, Fitzjarrald DR (1994) Seasonal and diurnal variations of coherent structures over a deciduous forest. Boundary-Layer Meteorol 69:43–69

Lu SS, Willmarth WW (1973) Measurements of the structure of the Reynolds stress in a turbulent boundary layer. J Fluid Mech 60:481–511

Mahrt L (2010) Computing turbulent fluxes near the surface: needed improvements. Agric For Meteorol 150:501–509

Maitani T, Shaw RH (1990) Joint probability analysis of momentum and heat fluxes at a deciduous forest. Boundary-Layer Meteorol 52:283–300

Paw UKT, Brunet Y, Collineau S, Shaw RH, Maitani T, Qiu J, Hipps L (1992) On coherent structures in turbulence above and within agricultural plant canopies. Agric For Meteorol 61:55–68

Poggi D, Porporato A, Ridolfi L, Albertson JD, Katul GG (2004) The effect of vegetation density on canopy sub-layer turbulence. Boundary-Layer Meteorol 111:565–587

Raupach MR, Finnigan JJ, Brunet Y (1996) Coherent eddies and turbulence in vegetation canopies: the mixing-layer analogy. Boundary-Layer Meteorol 78:351–382

Robinson SK (1991) Coherent motions in the turbulent boundary layer. Annu Rev Fluid Mech 23:601–639

Schlegel F, Stiller J, Bienert A, Maas HG, Queck R, Bernhofer C (2012) Large-eddy simulation of inhomogeneous canopy flows using high resolution terrestrial laser scanning data. Boundary-Layer Meteorol 142:223–243

Serafimovich A, Eder F, Hübner J, Falge E, Voss L, Sörgel M, Held A, Liu Q, Eigenmann R, Huber K, Ferro Duarte H, Werle P, Gast E, Cieslik S, Liu H, and Foken T (2011) ExchanGE processes in mountaineous regions (EGER). Documentation of the intensive oberservation period (IOP3) June, 13th–July, 26th. Arbeitsergebnisse/Department of Micrometeorology, University of Bayreuth. ISSN:1614-8916. no. 47, p 137

Serafimovich A, Thomas C, Foken T (2011b) Vertical and horizontal transport of energy and matter by coherent motions in a tall spruce canopy. Boundary-Layer Meteorol 140:429–451

Shaw RH, Tavangar J, Ward DP (1983) Structure of the reynolds stress in a canopy layer. J Clim Appl Meteorol 22:1922–1931

Sogachev A, Leclerc MY, Karipot A, Zhang G, Vesala T (2005) Effect of clearcuts on footprints and flux measurements above a forest canopy. Agric For Meteorol 133:182–196

Sogachev A, Leclerc MY, Zhang G, Rannik Ü, Vesala T (2008) CO_2 fluxes near a forest edge: a numerical study. Ecol Appl 18:1454–1469

Staebler RM, Fitzjarrald DR (2004) Observing subcanopy CO_2 advection. Agric For Meteorol 122:139–156

Staudt K, Foken T (2007) Documentation of recference data for the experimental areas of the Bayreuth Centre for Ecology and Environmental Research (BayCEER) at the Waldstein site. Arbeitsergebnisse, Department of Micrometeorology, University of Bayreuth. Bayreuth. ISSN:1614–8916, no. 35, p 37

Steiner AL, Pressley SN, Botros A, Jones E, Chung SH, Edburg SL (2012) Analysis of coherent structures and atmosphere-canopy coupling strength during the CABINEX field campaign. Atmos Chem Phys 11:11921–11936

Stull RB (1988) An introduction to boundary layer meteorology. Kluwer Academic Publishers, Dordrecht, p 666

Thomas C, Foken T (2005) Detection of long-term coherent exchange over spruce forest using wavelet analysis. Theor Appl Climatol 80:91–104

Thomas C, Foken T (2007a) Flux contribution of coherent structures and its implications for the exchange of energy and matter in a tall spruce canopy. Boundary-Layer Meteorol 123:317–337

Thomas C, Foken T (2007b) Organised motion in a tall spruce canopy: temporal scales, structure spacing and terrain effects. Boundary-Layer Meteorol 122:123–147

Thomas C, Mayer JC, Meixner F, Foken T (2006) Analysis of low-frequency turbulence above tall vegetation using a Doppler sodar. Boundary-Layer Meteorol 119:563–587

Torrence C, Compo GP (1998) A practical guide to wavelet analysis. Bull Am Meteorol Soc 79:61–78

Vickers D, Mahrt L (1997) Quality control and flux sampling problems for tower and aircraft data. J Atmos Oceanic Technol 14:512

Webb EK, Pearman GI, Leuning R (1980) Correction of flux measurements for density effects due to heat and water vapour transfer. Q J R Meteorol Soc 106:85–100

Wilczak J, Oncley S, Stage S (2001) Sonic anemometer tilt correction algorithms. Boundary-Layer Meteorol 99:127–150

Wilson K, Goldstein A, Falge E, Aubinet M, Baldocchi D, Berbigier P, Bernhofer C, Ceulemans R, Dolman H, Field C, Grelle A, Ibrom A, Law BE, Kowalski A, Meyers T, Moncrieff J, Monson R, Oechel W,

Tenhunen J, Valentini R, Verma S (2002) Energy balance closure at FLUXNET sites. Agric For Meteorol 113:223–243

Yang B, Morse A, Shaw R, Paw UKT (2006a) Large-eddy simulation of turbulent flow across a forest edge. Part II: momentum and turbulent kinetic energy budgets. Boundary-Layer Meteorol 121:433–457

Yang B, Raupach MR, Shaw RH, Paw UKT, Morse AP (2006b) Large-eddy simulation of turbulent flow across a forest edge. Part I: flow statistics. Boundary-Layer Meteorol 120:377–412

Zeeman MJ, Eugster W, Thomas CK (2013) Concurrency of coherent structures and conditionally sampled daytime sub-canopy respiration. Boundary-Layer Meteorol 146:1–15

Zhang G, Thomas C, Leclerc MY, Karipot A, Gholz HL, Binford M, Foken T (2007) On the effect of clearcuts on turbulence structure above a forest canopy. Theor Appl Climatol 88:133–137